

Graph Propagation and Distributed State Estimation Based on Local Modeling

Aleksandar A. Sarić

Department of Electrical and Computer Engineering
Tufts University
Medford, MA, USA
aleksandar.saric@tufts.edu

Alex M. Stanković

Department of Electrical and Computer Engineering
Tufts University
Medford, MA, USA
astankov@ece.tufts.edu

Abstract—We present a novel algorithm for distributed state estimation in power systems, based on graph theory and exchange of information between nodal entities in combination with local non-Jacobian based modeling. The bus-based power balance equations are used to generate a successively better estimate based on locally available data only, which is then sent out to adjacent graph vertices, so that information travels even to parts of the network that have fewer data collected. For this reason, full power system observability is not required, and this procedure could be applied even if parts of the system lack needed measurements. To demonstrate the effectiveness and scalability of the proposed algorithm, it is applied to both 14-bus and 300-bus test systems.

Index Terms— Power system, Distributed state estimation, Graph-based method, Local modeling, Non-Jacobian method.

I. INTRODUCTION

In the modern era, a highly reliable supply of electric energy has become the expected norm. No other infrastructure has such low tolerance for interruptions in service. For that reason, having a trustworthy gauge of the power system is essential.

In a traditional setting, all data that is collected is sent to a central location and from there the entire system is controlled. However, as power systems continue to increase in size and complexity, it has become clear that such an approach has many drawbacks. For instance, centralized state estimation (CSE) might involve the handling of the full system's matrix, which is easy to program, but costly in terms of resources for a large system. Also, the risk of creating bottlenecks during communication and security of the central agent are major issues.

Distributed state estimation (DSE) algorithms are designed to mitigate these problems [1], while at the same time trying to achieve a comparable level of accuracy. Monitoring the system from different physical locations and running calculations in parallel means not only higher speed, but also greater reliability because if one agent fails, others can continue functioning to a large degree.

The number of references in the DSE area in the last two decades highlights their importance for modern power system operation [2-14 and references therein]. In our context, all methods may be coarsely divided into two groups: 1) Jacobian based [2-10], and 2) non-Jacobian based [11-14]. Note that our proposed method is non-Jacobian-based. To a certain extent, the idea for this paper comes from [15], which analyses the problem of trilateration, but with similar constraints of limited

communication. Here, instead of localization in \mathbb{R}^m space of location coordinates, the goal is to determine the position for each bus in a space of state variables.

In this paper, we present a novel algorithm for calculating the condition of the power system using a combination of data-driven techniques and some fundamental equation-based models. Our algorithm starts with some fundamental power system equations and tries to estimate bus states (voltage magnitudes and angles) by forcing all solutions to satisfy these equations. At the same time, it is designed to use only locally available data, so that it can run in a distributed and iterative fashion, meaning that it has all the advantages offered by DSE algorithms. Furthermore, our approach allows us to bypass the standard conditions needed for CSE, such as observability requirements. Instead, our algorithm could work even if large portions of the system lack measurements.

The outline of the paper is as follows: in *Section II* we give the problem formulation, while *Section III* describes the algorithm and its steps in detail. In *Section IV* the proposed algorithm is applied to 14-bus and IEEE 300-bus test systems and many useful examples are provided. Finally, *Section V* presents conclusions. *Appendices A-C* give fundamental power system equations and inverse relations needed for the update step.

II. PROBLEM FORMULATION

We will analyze the power system with N_{bus} buses and N_{br} branches (lines or transformers). On top of it, we define an undirected graph as a higher level of abstraction, which will represent communication among graph entities. In the graph representation, each bus of the power system becomes a graph vertex, and there is a link between two vertices if there exists a branch connecting them in the original power system. We work with the assumption that communication is possible only between adjacent vertices. With such a setup, only local information is available when doing calculations in the current bus, so only a DSE technique could be applied.

For every bus in the power system, the estimation goal is to determine complex voltage (\underline{V}), which is represented by the voltage magnitude (V) and angle (θ). These are state variables, and their total number is $2N_{bus} - 1$ (for slack bus, the voltage angle has to be $\theta_{sl} = 0$, because it is used as a reference for all other bus angles). In addition, we assume that there are multiple sensors placed all over the power system, measuring different

This work has been supported by NSF under grant ECCS-1710944, by CURENT Engineering Research Center of the National Science Foundation and the Department of Energy under NSF Award Number EEC-1041877, by ONR under grant N00014-16-1-3028.

indirect quantities, such as active and reactive power injections in i th bus (P_i and Q_i , respectively), active and reactive power flows between i th and j th buses (P_{ij} and Q_{ij} , respectively), and the current flow between i th and j th buses (I_{ij}). These indirect quantities are then used to try to evaluate the values of state variables. Notice that our proposed algorithm does not require that we have all possible measurements mentioned here for every bus. Instead, the procedure will work properly even if many measurements are missing, but only up to a certain point (see *Section IV* for details). Furthermore, we assume it is possible that for some buses we also have direct measurements of quantities of interest (V and θ), albeit not for all of them and with some level of uncertainty (represented by a noise).

III. ALGORITHM DEVELOPMENT

For any power system topology, the active/reactive power bus balance equations must be satisfied. They are given in *Appendix A* by (A3), (A4), (A6), and (A7) (note that current measurements are not used—but the extension is straightforward). Notice that these equations relate measurements of indirect quantities (P_i, Q_i, P_{ij}, Q_{ij}) (denoted as *indirect measurements*), state variables (V, θ) (denoted as *direct measurements*), and system parameters (G, B, Y, ψ). They are highly nonlinear and general, in the sense that they describe the nonlinear (AC) case. In case when only a linear (DC) model is of interest, certain approximations can be used, which would result in simpler, linear equations—see (A8) and (A9). The algorithm will be developed both for linear (DC-based) and nonlinear (AC-based) models. In both cases, the idea is to find such state variable values so that they are consistent with obtained measurements and power balance equations are satisfied. The flow chart of the proposed algorithm is shown in Figure 1.

The algorithm starts with collecting all the available measurements and preprocessing data (*Step 1*). In *Step 2*, the initialization is done for all state variables [only vector θ for linear (DC) model, or both V and θ for nonlinear (AC) model]. One way (simplest in this context) is to use measurements of these quantities if they are available, and if not, then simply assigning the flat start initial solution ($V_0 = 1$ pu and $\theta_0 = 0$). As it turns out, such an approach works well for the linear (DC) model. However, for nonlinear (AC) based case, it is well-known that there are multiple power flow solutions [16], and the algorithm could converge to some local optimum, which suggests the importance of starting from the best possible initial condition. In general, two approaches can be applied: 1) *operation-based*, where the initial conditions can be final state estimates from the previous time instant [respecting the slow changes in network conditions for typical times for SE execution (3-10 sec)], or 2) *mathematically-based*, where the initial solutions can be estimated from local indirect measurements with lowest variances.

In the next step (*Step 3*), the order in which bus estimates will be updated is determined. It makes sense and is empirically proven with simulations that it is best to start by first updating those buses that have direct measurements of state variables (V and θ), and later update remaining buses sorted by the number of indirect measurements (in descending order).

Step 4 is the update of state variables and is the heart of the algorithm. It is done in a way to ensure that power balance equations become satisfied. In each iteration, the goal is to modify

them based on available measurements and state variables in neighboring graph vertices (buses), to minimize the inconsistencies between the left and right side of power balance equations. This update is *Step 4a* and will be described in detail below. In *Step 4b*, these newly calculated values are sent out to neighboring graph vertices, so that the most up-to-date estimates are used when doing the update for those buses.

Step 4a and *Step 4b* are repeated as long as the convergence criterion is not satisfied. In this case, the criterion was chosen to be the change of Mean Squared Error (MSE) between two successive iterations, the threshold of MSE, and/or maximum allowed number of iterations.

A. Update of state variables for linear (DC) model

To perform the update of state variables (*Step 4a*), we start with bus active power balance and branch active power flow equations [(A8) and (A9)] and need to derive inverse expressions for θ_i in i th bus, which could be used if all other variables are assumed to be known

$$\mathbf{z}_i^{\text{indirect}} = f(\theta_i, \theta_j, \mathbf{p}) \Rightarrow \theta_i = f^{-1}(\mathbf{z}_i^{\text{indirect}}, \theta_j, \mathbf{p}) \quad (1)$$

In this symbolic equation (1) for linear (DC-based) model, $\mathbf{z}_i^{\text{indirect}}$ represents any indirect measurement available for i th bus (active power injection and power flows to N_{α_i} neighboring buses: $\mathbf{z}_i^{\text{indirect}} = \{P_i^m, P_{i1}^m, P_{i2}^m, \dots, P_{i,N_{\alpha_i}}^m\}$), θ_j is the estimate of voltage angle in j th bus that is neighbor to bus with angle θ_i , and \mathbf{p} is a set of system parameters (typically represented by the system admittance matrix $\mathbf{Y} = \mathbf{G} + j\mathbf{B}$ —see *Appendix A*).

More important than f is the inverse relation f^{-1} , which is used to find $\theta_i(\mathbf{z}_i^{\text{indirect}})$, an estimate of angle based on that particular measurement type. A way to find angles from power injection (P_i) is shown in (B1). Similarly, (B2) is used to predict bus voltage angle from active power flow P_{ij} . If the direct measurement of bus voltage angle (θ_i^m) is also present, it will be used in (2) without any modification.

For one direct ($\mathbf{z}_i^{\text{direct}} = \{\theta_i^m\}$) and $m = 1, 2, \dots, N_i^{\text{indirect}}$ indirect measurements, the predicted value for voltage angle in i th bus is calculated as the weighted average of individual predictions

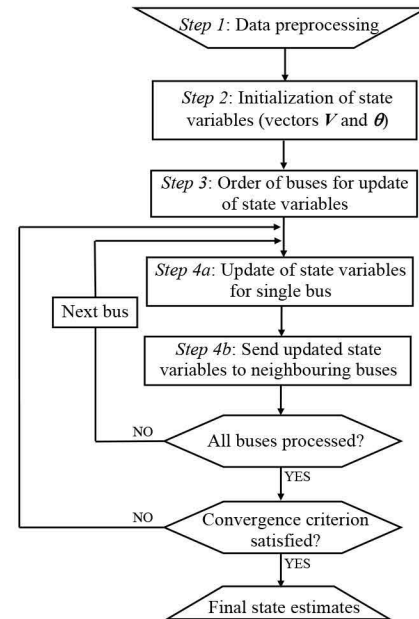


Figure 1. Flow chart of the proposed algorithm

$$\theta_i = \frac{w_{\theta_i} \theta_i^m + \sum_{m=1}^{N_i^{\text{indirect}}} w_m \theta_i(z_{i,m}^{\text{indirect}})}{w_{\theta_i} + \sum_{m=1}^{N_i^{\text{indirect}}} w_m} \quad (2)$$

where:

m – the type of measured value (in superscript);

$$w_m = 1/\sigma_m; w_{\theta_i} = 1/\sigma_{\theta_i};$$

$\sigma_m, \sigma_{\theta_i}$ – variance of the m th indirect measurement and variance of the direct voltage angle measurement in i th bus, respectively.

Eq. (2) generates an estimate by combining all available information related to the i th bus. If any measurement is not available, it is simply removed from (2). Weights are defined so that more emphasis is given to measurements with low variance.

To better understanding the proposed idea, the update step is illustrated in Figure 2. It shows that for the linear (DC) model the bus voltage angle estimates are along the line, i.e. one-dimensional (1D) problem. Yellow areas show an interval of the expected solution. For buses with direct measurements, these values will be used as the initial solution $\theta_{i0} = \theta_i^m$, and the interval of expected final estimates is small (acts as an anchor point). For the remaining buses, where direct measurements are not available, the initial values are set to zero $\theta_{i0} = 0$; $i = 1, 2, \dots, N_{\text{bus}}$, and we have wider intervals and it is expected that the final estimates will move significantly from initial ones. At each iteration, a new estimate is made and the point moves along the line toward the final estimates.

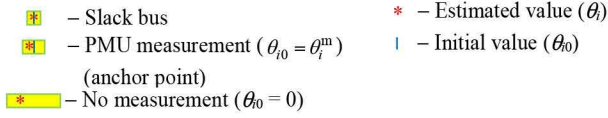


Figure 2. Illustration of one-dimensional update step for bus voltage angles

B. Update of state variables for nonlinear (AC) model

In the case of the nonlinear (AC) model, things conceptually stay the same, but power equations are now nonlinear and more complex, and for each bus, state variables are not only angles (θ_i), but also voltage magnitudes (V_i). For the update of state variables, we need to derive inverse expressions for elements of vectors $\boldsymbol{\theta}$ and \mathbf{V} , which could be used if all other variables are assumed to be known

$$\mathbf{z}_i^{\text{indirect}} = f(\theta_i, \theta_j, V_i, V_j, \mathbf{p}) \Rightarrow \theta_i, V_i = f^{-1}(\mathbf{z}_i^{\text{indirect}}, \theta_j, V_j, \mathbf{p}) \quad (3)$$

Just like before, $\mathbf{z}_i^{\text{indirect}}$ represents indirect measurements, but in this nonlinear (AC-based) model, it also includes reactive power injections and power flows, hence $\mathbf{z}_i^{\text{indirect}} = \{P_i^m, Q_i^m, P_{i1}^m, P_{i2}^m, \dots, P_{i,N_{a_i}}^m, Q_{i1}^m, Q_{i2}^m, \dots, Q_{i,N_{a_i}}^m\}$. The expanded form of function f can be found in *Appendix A*, (A3), (A4), (A6), and (A7).

Inverse relation f^{-1} has to be determined both for voltage magnitude and angle. In the case of V_i , this is straightforward, because in all four equations it comes down to solving quadratic equations (see *Appendix C*). When doing this for θ_i , things get a bit more complicated because of the nonlinearity of trigonometric functions and the fact that θ_i may be present in multiple terms. To get explicit expressions, one needs to use trigonometric identities. For example, to calculate θ_i when measurement

P_i or Q_i is given, (B3)-(B6), and (B7) can be used, respectively. To calculate θ_i from P_{ij} or Q_{ij} , (B8) and (B9) can be used.

For two direct measurement ($\mathbf{z}_i^{\text{direct}} = \{\theta_i^m, V_i^m\}$) and estimates obtained using inverse formulas f^{-1} , the predicted value for voltage angle in i th bus is still given by (2), while the predicted value for voltage magnitude in i th bus is

$$V_i = \frac{w_{V_i} V_i^m + \sum_{m=1}^{N_i^{\text{indirect}}} w_m V_i(z_{i,m}^{\text{indirect}})}{w_{V_i} + \sum_{m=1}^{N_i^{\text{indirect}}} w_m} \quad (4)$$

where $w_{V_i} = 1/\sigma_{V_i}$, and σ_{V_i} is the variance of the voltage magnitude measurement in i th bus.

This case can also be visualized as in Figure 3. The space in which we search for state estimates of i th bus is now two-dimensional (2D). Each bus will exchange information with its neighbors about their current estimates and use that data together with measurements to update itself and move in this 2D state space.

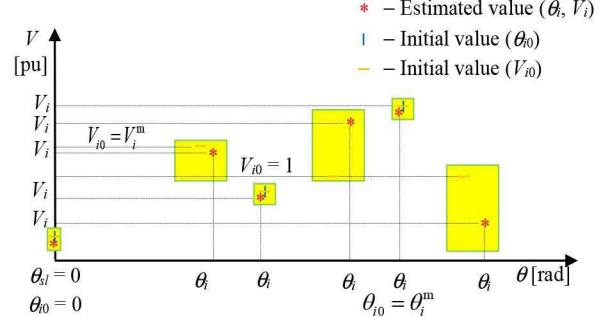


Figure 3. Illustration of two-dimensional update step for bus voltage angles and magnitudes

IV. APPLICATION

To demonstrate the effectiveness of the proposed algorithm, Matlab simulations were performed on 14-bus and IEEE 300-bus test systems [17]. Sets of direct and indirect measurements are generated by a power flow solution with/without additional measurement noise. These values will be used as a benchmark to all other results, including: 1) estimates of voltage magnitudes and angles in all buses, and 2) calculated indirect quantities (active/reactive power injections and flows). Obtained results are compared with the traditional Weighted-Least Square (WLS) based CSE algorithm, using the same set of measurements. To assess the quality of estimates, we will use MSE of difference between measurements and corresponding estimates for both CSE and DSE algorithms.

TABLE I: AN OVERVIEW OF FULL MEASUREMENT SETS FOR BOTH 14-BUS AND 300-BUS TEST SYSTEMS FOR BOTH LINEAR (DC) AND NONLINEAR (AC) MODELS

	14-bus test system		300-bus test system	
	DC model	AC model	DC model	AC model
N_{bus}	14		300	
N_{br}	20		409	
θ_i^m	13*	13	299	299
V_i^m	–	14	–	300
P_i^m	14	14	300	300
Q_i^m	–	14	–	300
P_{ij}^m	20	40	409	409
Q_{ij}^m	–	40	–	409
Total number of measurements	47	135	1008	2317

* Notice that in the slack bus $\theta_{sl} = 0$

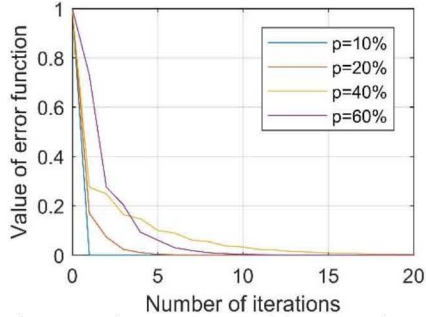


Figure 4. The convergence of the proposed DC-based DSE algorithm for different percentage levels of unavailable measurements (p)—the 14-bus test system.

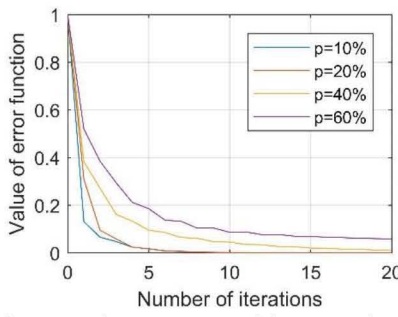


Figure 5. The convergence of the proposed DC-based DSE algorithm for different percentage levels of unavailable measurements (p)—the 300-bus test system.

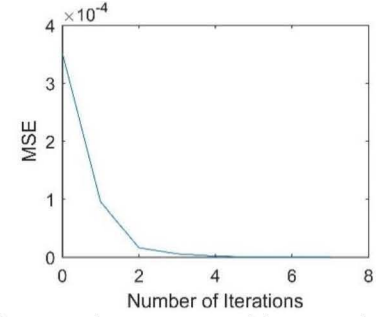


Figure 6. The convergence of the proposed AC-based DSE algorithm for the 14-bus test system.

An overview of the full measurement sets for both test systems and linear (DC) and nonlinear (AC) models is shown in Table I.

Following values of measurement variances (σ) are used for the simulation: 1) voltage magnitudes (10^{-2}), 2) voltage angles (10^{-3}), and 3) active/reactive power injections/flows (10^{-1}).

A. Linear (DC) Model for 14-bus and 300-bus Test Systems

In this part, we will assume that measurements are accurate (no noise is added), but many of them are missing (they are eliminated randomly). Convergence properties of the proposed DSE algorithm for different percentage levels of unavailable measurements (p) from Table I (values in row ‘Total number of measurements’) are shown in Figure 4 and Figure 5 (for 14 and 300-bus test system, respectively). The MSE for each case is normalized so that all graphs start at value 1. As expected, with an increase of missing measurements, the convergence rate decreases, but more important is the fact that even in these unfavorable conditions algorithm converges to expected values and MSE decreases with each iteration.

The next set of simulations is performed with a noise introduced for the 300-bus test system. We assume that all indirect quantities are measured (active power injection and flow measurements), and there are no measurements of direct quantities (voltage angles, except for slack angle used as a reference, or $\theta_{sl} = 0$). Table II compares calculated MSE as the noise variance σ changes. Noise is Gaussian with zero mean.

TABLE II: CALCULATED MSE AS A FUNCTION OF MEASUREMENT NOISE FOR THE PROPOSED DC-BASED DSE ALGORITHM [300-BUS TEST SYSTEM]

Noise [%]	MSE
0	0.0000
2	0.2128
5	0.4418
10	1.2751
15	1.7589

B. Nonlinear (AC) Model for 14-bus Test System

Detailed results for the 14-bus test system obtained by the nonlinear (AC) model for the percentage level of unavailable measurements $p = 20\%$ are shown in Table III. The measurement set is obtained from the power flow solution with additional noise of 5 %. The convergence of the proposed DSE algorithm is shown in Figure 6. From Figure 6 we conclude that the proposed DSE algorithm converges in only four iterations.

TABLE III: MEASURED STATE VARIABLES AND RESULTS COMPARISON FOR THE PROPOSED DSE AND WLS-BASED CSE FOR NONLINEAR (AC) MODEL [14-BUS TEST SYSTEM]

Bus i	Voltage angle (θ_i) [rad]			Voltage magnitude (V_i) [pu]		
	Measured	Estimation (Proposed DSE)	Estimation (WLS-based CSE)	Measured	Estimation (Proposed DSE)	Estimation (WLS-based CSE)
1	0.0000	0.0000	0.0000	1.0576	1.0600	1.0600
2	-0.0347	-0.3501	-0.3501	1.0326	1.0350	1.0350
3	-0.1404	-0.1374	-0.1374	0.9866	0.9889	0.9889
4	-0.0766	-0.0761	-0.0761	1.0292	1.0315	1.0315
5	-0.0557	-0.0553	-0.0553	1.0378	1.0400	1.0400
6	-0.0677	-0.0692	-0.0692	1.0417	1.0435	1.0435
7	-0.0530	-0.0523	-0.0523	1.0414	1.0433	1.0433
8	0.0115	0.0103	0.0103	1.0790	1.0800	1.0800
9	-0.0805	-0.0797	-0.0797	1.0250	1.0273	1.0273
10	-0.0734	-0.0728	-0.0728	1.0278	1.0305	1.0305
11	-0.0454	-0.0461	-0.0460	1.0545	1.0570	1.0570
12	-0.0782	-0.0786	-0.0786	1.0396	1.0406	1.0406
13	-0.0779	-0.0788	-0.0787	1.0490	1.0500	1.0500
14	-0.0973	-0.0972	-0.0972	1.0179	1.0189	1.0189

C. Convergence Characteristics of Linear (DC) Model for 300-bus Test System

In Table IV we give a comparison of the convergence results for DSE and WLS-based CSE for the linear (DC) model. From the presented results we can conclude that the proposed DSE gives better results in cases with an increase of missing measurements (with lower computation time). For $p = 40\%$ and $p = 60\%$, the WLS-based CSE model fails to provide a solution, due to the gain matrix being close to singular ($\mathbf{H}^T \mathbf{R}^{-1} \mathbf{H}$, where \mathbf{H} is the Jacobian matrix, $\mathbf{R} = \text{diag}\{1/\sigma_m^2\}$ is the measurement covariance matrix, and σ_m is the variance of m th measurement), and the unobservability of some buses (no adjacent measurements).

TABLE IV: COMPARISON OF THE RESULTS FOR BOTH PROPOSED DSE AND WLS-BASED CSE ALGORITHMS AND 300-BUS TEST SYSTEM [OBTAINED BY LINEAR (DC) MODEL]

p [%]	Proposed DSE algorithm			WLS-based CSE algorithm	
	MSE	Number of iterations	CPU* [s]	MSE	CPU [s]
0	0.000639	3	0.1347	0	0.266
10	0.014770	3	0.1275	0.254	0.260
20	0.121720	3	0.1240	0.247	0.181
40	0.223792	3	0.1202	NaN	0.156
60	0.636814	3	0.1144	NaN	0.063

*CPU time is measured at a machine with the following characteristics: Intel(R) Core(TM) i7-6860HQ CPU @ 2.70 GHz, 64-bit Operating System, 32 GB RAM.

V. CONCLUSION

This paper presented a distributed state estimation algorithm, which combines the graph-based topology properties, available measurements, and physics-based active and reactive power equations. As simulations show, the proposed algorithm quickly (typically less than 10 iterations) converges to the equilibrium point and is also able to deal with a high percentage of missing measurements. Moreover, it is robust to noise and does not require full network observability, so can be applied in cases when centralized state estimation cannot be used.

For future work, several directions seem promising. Firstly, better initial conditions could be used instead of a flat start initial solution to increase the rate of convergence. Of course, to keep the algorithm fully distributed, the improved initial solution must be based on local measurements only. Another line of work could include using the update step as the local nonlinear optimization problem and comparing properties with the current method. Finally, with some modifications, the proposed algorithm could also be used to analyze cases when the blackout of large portions of the power system occurs, and identify boundaries that separate unidentifiable areas.

REFERENCES

- [1] A. Gómez-Expósito, *et al.*, "A taxonomy of multi-area state estimation methods," *Electric Power Sys. Research*, vol. 81, no. 4, pp. 1060–1069, Apr. 2011.
- [2] L. Zhao, A. Abur, "Multi-area state est. using synchronized phasor measurements," *IEEE Trans. Power Syst.*, vol. 20, no. 2, pp. 611–617, May 2005.
- [3] R. Ebrahimi, R. Baldick, "State estimation distributed processing," *IEEE Trans. Power Syst.*, vol. 15, no. 4, pp. 1240–1246, Nov. 2000.
- [4] L. Xie, D.H. Choi, S. Kar, H.V. Poor, "Fully distributed state estimation for wide-area monitoring systems," *IEEE Trans. Smart Grid*, vol. 3, no. 3, pp. 1154–1169, Sep. 2012.
- [5] V. Kekatos, G.B. Giannakis, "Distributed robust power system state estimation," *IEEE Trans. Power Syst.*, vol. 28, no. 2, pp. 1617–1626, May 2013.
- [6] A. Minot, Y. M. Lu, N. Li, "A distributed Gauss-Newton method for power system state estimation," *IEEE Trans. Power Syst.*, vol. 31, no. 5, pp. 3804–3815, Sep. 2016.
- [7] Y. Guo, L. Tong, W. Wu, H. Sun, B. Zhang, "Hierarchical multi-area state estimation via sensitivity function exchanges," *IEEE Trans. Power Syst.*, vol. 32, no. 1, pp. 442–453, Jan. 2017.
- [8] S. Xia, *et al.*, "Distributed state estimation of multi-region power system based on consensus theory," *Energies*, vol. 12, no. 5, pp. 1–16, 2019.
- [9] J. Le, *et al.*, "Multi-area distributed state estimation strategy for large-scale power grids," *IEEE Access*, vol. 7, pp. 117580–117590, Aug. 2019.
- [10] T. Chen, *et al.*, "A distributed robust power system state estimation approach using *t*-distribution noise model," *IEEE Systems Journal*, pp. 1–11. To be published. DOI: 10.1109/JSYST.2020.2987612.
- [11] W. Jiang, *et al.*, "Diakoptics state estimation using phasor measurement units," *IEEE Trans. Power Syst.*, vol. 23, no. 4, pp. 1580–1589, Nov. 2008.
- [12] A. Sharma, S.C. Srivastava, S. Chakrabarti, "Multi-area state estimation using area slack bus angle adjustment with minimal data exchange," *IEEE PES General Meeting*, pp. 1–5, Jul. 2013.
- [13] W. Zheng, *et al.*, "Distributed robust bilinear state estimation for power systems with nonlinear measurements," *IEEE Trans. Power Syst.*, vol. 32, no. 1, pp. 499–509, Jan. 2017.
- [14] M. Cosovic, D. Vukobratovic, "Distributed Gauss-Newton method for state estimation using belief propagation," *IEEE Trans. Power Syst.*, vol. 34, no. 1, pp. 648–658, Jan. 2019.
- [15] U.A. Khan, S. Kar, J.M.F. Moura, "Linear theory for self-localization: Convexity, barycentric coordinates, and Cayley-Menger determinants," *IEEE Access*, vol. 3, pp. 1326–1339, Aug. 2015.
- [16] T. Chenand, D. Mehta, "On the network topology dependent solution count of the algebraic load flow equations," *IEEE Trans. Power Syst.*, vol. 33, no. 2, pp. 1451–1460, Mar. 2018.
- [17] R. Christie, *14-bus and 300-bus Power Flow Test Cases*, University of Washington. www2.ee.washington.edu/research/pstca/pf14/pg_tca14bus.htm

APPENDIX A: FUNDAMENTAL POWER SYSTEM EQUATIONS

The bus-branch current injection model is

$$\underline{I} = \underline{Y}V \quad (A1)$$

and the apparent power in *i*th bus ($i = 1, 2, \dots, N_{bus}$) is

$$S_i = P_i + jQ_i = \underline{V}_i \underline{I}_i^* = V_i^2 \underline{Y}_{ii}^* + \underline{V}_i \sum_{j \in \alpha_i} \underline{Y}_{ij}^* \underline{V}_j^* \quad (A2)$$

From (A2), the active and reactive power injections respectively are:

$$P_i = V_i^2 G_{ii} + V_i \sum_{j \in \alpha_i} [V_j G_{ij} \cos(\theta_i - \theta_j) + V_j B_{ij} \sin(\theta_i - \theta_j)] \quad (A3)$$

$$Q_i = -V_i^2 B_{ii} + V_i \sum_{j \in \alpha_i} [V_j G_{ij} \sin(\theta_i - \theta_j) - V_j B_{ij} \cos(\theta_i - \theta_j)] \quad (A4)$$

The apparent power flow in a branch between *i*th and *j*th buses is

$$S_{ij} = V_i^2 \underline{Y}_{ij}^0 + \underline{V}_i \underline{I}_j^* = V_i^2 \underline{Y}_{ij}^0 - \underline{V}_i \underline{Y}_{ij}^* (V_i^* - V_j^*) \quad (A5)$$

or active and reactive power flows respectively are

$$P_{ij} = -V_i^2 (G_{ij} - G_{ij}^0) + V_i V_j Y_{ij} \cos(\theta_i - \theta_j - \psi_{ij}) \quad (A6)$$

$$Q_{ij} = V_i^2 (B_{ij} - B_{ij}^0) + V_i V_j Y_{ij} \sin(\theta_i - \theta_j - \psi_{ij}) \quad (A7)$$

For linear (DC) formulation, from (A3) and (A6), the active power injections and power flows respectively are

$$P_i = \sum_{j \in \alpha_i} [B_{ij} (\theta_i - \theta_j)] \quad (A8)$$

$$P_{ij} = B_{ij} (\theta_i - \theta_j) \quad (A9)$$

Notice that in (1) and (3), eqs. (A3), (A4), (A6), (A7), (A8), (A9) are symbolically denoted as *f*.

APPENDIX B: UPDATE OF VOLTAGE ANGLES (STEP 3A)

For linear (DC) formulation, from (A8) and (A9), we have

$$\theta_i (P_i^m) = \frac{P_i^m + \sum_{j \in \alpha_i} B_{ij} \theta_j}{\sum_{j \in \alpha_i} B_{ij}} \quad (B1)$$

$$\theta_i (P_{ij}^m) = \frac{P_{ij}^m}{B_{ij}} + \theta_j \quad (B2)$$

For nonlinear (AC) formulation in (A3) and (A4), one needs to use trigonometric identities to get explicit inverse expressions. The final result for (A3) is

$$\theta_i (P_i^m) = \arcsin\left(\frac{c}{\sqrt{c_1^2 + c_2^2}}\right) - \arctan\left(\frac{c_2}{c_1}\right) \quad (B3)$$

where

$$c = \frac{P_i^m - V_i^2 G_{ii}}{V_i} \quad (B4)$$

$$c_1 = \sum_{j \in \alpha_i} V_j G_{ij} \sin \theta_j + V_j B_{ij} \cos \theta_j \quad (B5)$$

$$c_2 = \sum_{j \in \alpha_i} V_j G_{ij} \cos \theta_j - V_j B_{ij} \sin \theta_j \quad (B6)$$

The final result for (A4) is

$$\theta_i (Q_i^m) = \arcsin\left(\frac{c}{\sqrt{c_1^2 + c_2^2}}\right) - \arctan\left(\frac{c_2}{c_1}\right) \quad (B7)$$

where *C*, *C*₁, and *C*₂, can be determined from (A4) [similarly as in (B4)–(B6) for active power injections].

For (A6) and (A7), it can be done relatively easily by finding the inverse of sine or cosine functions, taking into account the possibility of multiple solutions, respectively

$$\theta_i (P_{ij}^m) = \arccos\left(\frac{P_{ij}^m + V_i^2 (G_{ij} - G_{ij}^0)}{V_i V_j Y_{ij}}\right) + \theta_j + \psi_{ij} \quad (B8)$$

$$\theta_i (Q_{ij}^m) = \arcsin\left(\frac{Q_{ij}^m - V_i^2 (B_{ij} - B_{ij}^0)}{V_i V_j Y_{ij}}\right) + \theta_j + \psi_{ij} \quad (B9)$$

Notice that in (1) and (3), eqs. (B1)–(B3), (B7)–(B9) are symbolically denoted as *f*⁻¹.

APPENDIX C: UPDATE OF VOLTAGE MAGNITUDES (STEP 3A)

First, we note that this update is applied only for the nonlinear (AC) DSE model.

From (A3), (A4), (A6), and (A7) we conclude that the voltage update in *i*th bus (*V*_{*i*}) is the solution of a quadratic equation

$$aV_i^2 + bV_i + c = 0 \quad (C1)$$

where the coefficients *a*, *b*, and *c* can be identified from the above-mentioned equations (A3), (A4), (A6), and (A7).